VORTEX SHEDDING NOISE REDUCTION OF A MIXED FLOW FAN: EXPERIMENTAL AND NUMERICAL INVESTIGATION

Michael J. COLLISON, Ryan N. STIMPSON,
Ludovic DESVARD

*DYSON Ltd, Aeroacoustic Research Team, RDD, Tetbury Hill,
Malmesbury, SN160RP, United-Kingdom*

SUMMARY

The work presented in this paper investigates the influence of the trailing edge on the noise generated by a low Reynolds number mixed flow compressor. Several types of trailing edge details have been evaluated in terms of aerodynamic performance and noise. Both numerical and experimental methods have been performed to assess the different designs. The Sharpness, a psychoacoustic metric, is used to evaluate the effect of the vortex shedding on the sound quality. A 'wavy' (sinusoidal) trailing edge geometry shows an improvement in sound quality when compared with straight trailing edge designs. Furthermore, this design does not affect the aerodynamic performance.

INTRODUCTION

Sound quality for domestic appliances is paramount [1, 2]. In most air moving devices, the noise emanating from the compressor represents a significant acoustic source. The work presented in this paper was carried out to assess the influence of the trailing edge (TE) design on the noise generated by a low Reynolds number mixed flow compressor ($Re < 10^6$) used in the base of the Dyson Air Multiplier[TM] desk fan, [3].

The noise generated from a trailing edge can be split into two sources (illustrated in Figure 1):

- Turbulent Boundary Layer Trailing Edge (TBL-TE) noise – This is generated by the turbulent boundary layer passing over the trailing edge.
- Blunt Trailing Edge (BTE) noise – This is generated from von Kármán vortex shedding over the blunt trailing edge.
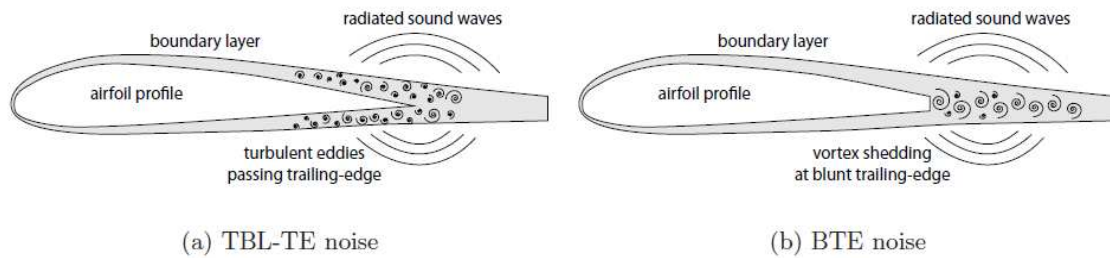
Figure 1: Illustration of trailing edge noise sources for a sharp (a) and a blunt (b) trailing edge (from [4]).

TBL-TE noise is mostly broadband; however BTE noise is narrowband, centred on a dominant frequency which can be determined from the Strouhal relationship as follows:

$$St = \frac{fL}{V} \tag{1}$$

Where f is the vortex shedding frequency, L is a characteristic length, and V is the local flow velocity. The Strouhal number (St) is non-dimensional and, for most low Reynolds numbers airfoils the vortex shedding will appear at approximately $St = 0.2$, [5].

Low Reynolds number flows on airfoils with blunt trailing edges are known to produce vortex shedding, however the laminar or turbulent boundary layer regime is found to affect the noise generated as described by [6, 7]. A mixed flow compressor blade may act more like a flat plate, potentially changing its associated Strouhal number, but the blunt trailing edge vortex shedding phenomenon is still produced by the same flow physics. Moreau, in [8], has shown that the vortex shedding phenomenon can occur at significantly different Strouhal numbers of around 0.1.

Pröbsting, in [4], explains that a trailing edge is considered blunt if the ratio between the thickness and the displacement thickness is greater than 0.3. Below this limit, blunt trailing edge noise is deemed to be insignificant. For the thinnest trailing edge blade studied in this paper, the ratio is >>0.3. It should therefore be considered blunt, and consequently will create significant BTE noise.

TBL-TE noise is always generated, and is the main focus of current serration trailing edge treatments which aim to improve mixing. Applied to a turbofan blade, [9], the serration decreases the noise by reducing the associated velocity non-uniformities of the wake passing the stator leading edge. Another example is the CFM56 gas-turbine engine chevrons on the core ducting trailing edge which are found to improve the shear layer mixing at the exhaust and reduce the associated loudness, [10].

For high Reynolds number large scale machines, the trailing edge noise is generally only TBL-TE noise, because the large scale allows for sharp trailing edges. However at the smaller scale of low Reynolds number, the relative size of the trailing edge to the chord is likely to be higher, and this means that BTE noise becomes more dominant.

Compared with the high Reynolds number gas turbine engine applications, the effect of serrations on lower Reynolds number wind turbines for example is different. Instead of the longitudinal vortices produced by the serrations increasing the mixing of wakes or shear layers, they have the effect of breaking down the von Kármán vortex sheets produced by the blunt trailing edge. The suppression of the von Kármán vortex sheets results in a reduction in the vortex shedding noise. There are numerous examples of serrated (otherwise known as 'saw tooth') trailing edge patents for wind turbines [11, 12].

The non-dimensional coefficients associated with the design point of the mixed flow compressor under investigation are:

$$Re_{Chord} \approx 100{,}000 \qquad \phi = \left(\frac{Q}{ND^3}\right)_{exit} = 0.037 \qquad \psi = \left(\frac{\Delta p_0}{\rho N^2 D^2}\right)_{exit} = 0.043$$

Where Re_{Chord} is the Reynolds number defined by the chord and the relative velocity at the outlet both at mid-span, ϕ is the flow coefficient and ψ is the head coefficient. Q is the volumetric flow rate, N is the rotational speed, D is the wheel diameter, Δp_0 is the total pressure rise and ρ is the air density. Three trailing edge geometries are evaluated numerically and experimentally in this paper. An illustration of the three configurations is shown in Figure 2.

Figure 2: Illustration of the three trailing edge geometries, (left) thin straight, (middle) thick straight and (right) wavy.

In the context of the mixed flow compressor under investigation, the thickness (t) and the relative velocity (V_{Rel}) at the operating point mass flow rate vary along the blade span as described in Table 1. The relative velocities are extracted from the numerical approach described in the next section.

Table 1: Details of the different trailing edge geometries.

Span location	Thin straight TE		Thick straight TE		Wavy TE	
	t (mm)	V_{Rel} (m/s)	t (mm)	V_{Rel} (m/s)	t (mm)	V_{Rel} (m/s)
Hub	0.40	19.8	1.00	20.1	0.40	19.5
Mean	0.35	22.4	0.95	23.6	0.35	22.4
Tip	0.30	20.2	0.90	20.2	0.30	19.9

NUMERICAL APPROACH

The different trailing edge geometries have been assessed using Computational Fluid Dynamics (CFD). This investigation was carried out in ANSYS Fluent 15.0. The mesh was created using geometry files generated in Concepts NREC AxCent and meshed in ANSYS TurboGrid 15.0. The simulation was solved on a desktop PC using 10 cores.

The key features of the mesh were to have a dimensionless wall distance (y+) around the blade of 1 and to refine the mesh in the wake region to capture any vortex shedding or wake structures accurately. These specifications resulted in a single passage mesh of the mixed flow fan blade with approximately 13.5 million cells. A detailed view of the mesh is shown in Figure 3.
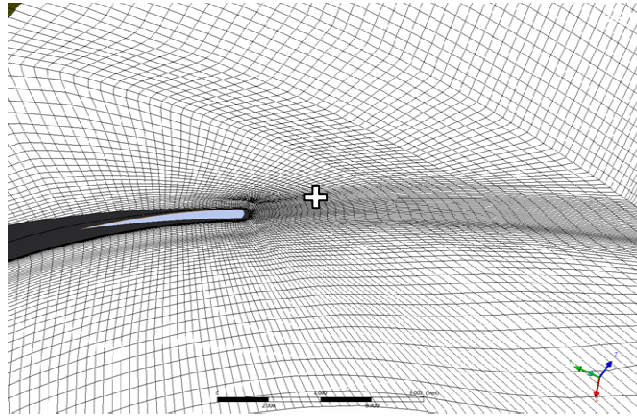
Figure 3: Trailing edge, wake mesh detail and approximate location of wake pressure probe point (white cross).

The solution is initialised using Full Multigrid (FMG) method and the SST k-ω turbulence model with a mass flow inlet and pressure outlet boundary. The mass flow inlet is set to the design point mass flow whilst the pressure outlet is set to zero. The whole domain is set with reference frame rotation at the design rotation speed. Following the FMG initialisation, the solution was run until convergence of the inlet pressure was observed, such that the inlet boundary could be switched to a pressure inlet boundary whilst maintaining approximately the mass flow through the system.

Once satisfied that the initial steady state solution was converged, the solution was switched to detached eddy simulation (DES) SST k-ω and to transient. A time step of 2e-6 s was chosen to ensure good resolution of the expected vortex shedding frequency. A probe point located in the wake region was monitored to determine a vortex shedding frequency. To induce oscillation into the flow, the inlet pressure boundary was decreased for 10 time steps to a moderately lower value, and then re-established at its original design condition value. This was enough to induce the vortex shedding on the blade.

The vortex shedding can be seen on the velocity contours shown in Figure 4. An indication of the vortex shedding could also be observed using the Q-criterion (spatial visualisation of vortices) in the same region as shown in Figure 5.
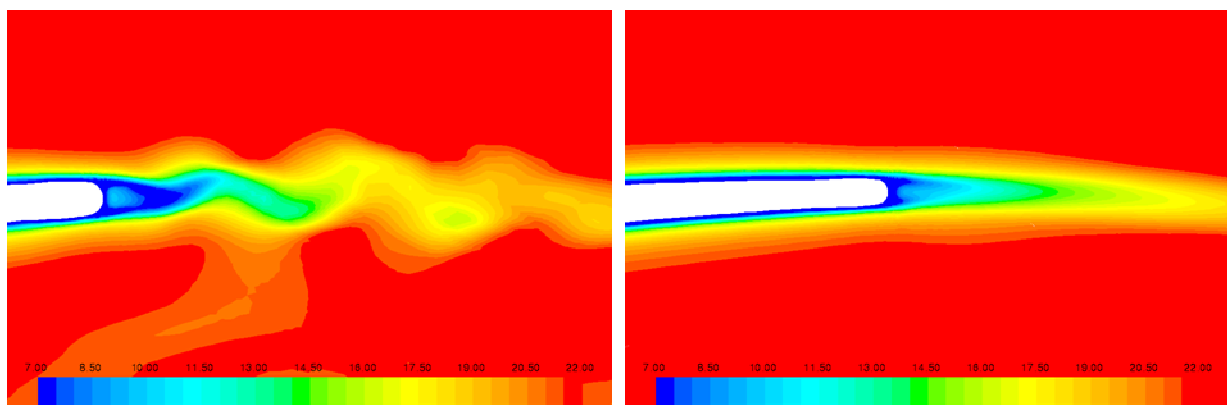

Figure 4: Velocity contour for (left) the thin TE and (right) the wavy TE.
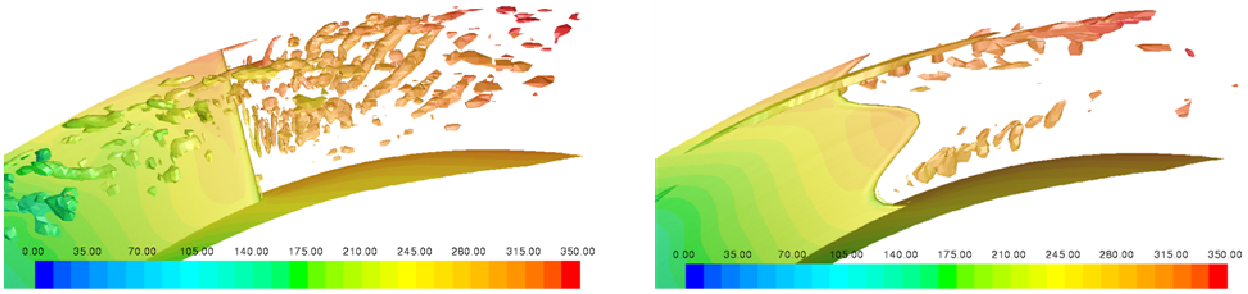
Figure 5: Q-criterion for (left) the thin TE and (right) the wavy TE.

A more objective representation of the vortex shedding can be obtained by observing the wake pressure fluctuation in the frequency domain. At the probe point (illustrated in Figure 3), the time series is extracted and the spectrum in frequency domain is calculated, the resulting signatures for the three configurations are shown in Figure 6.
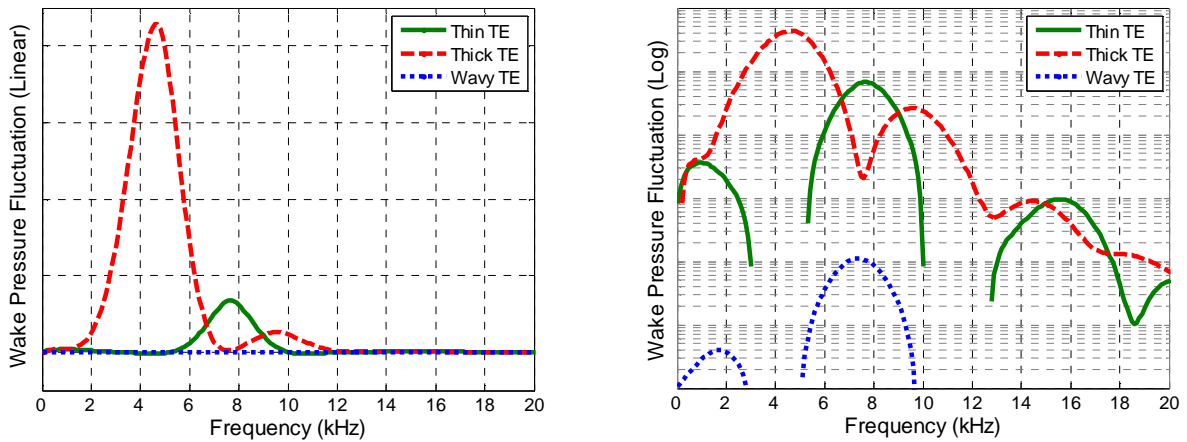

Figure 6: Spectra of the wake pressure fluctuation, (left) linear and (right) logarithmic magnitude.

For both straight TE geometries, the vortex shedding frequencies are observed around 7.7 kHz and 4.7 kHz for the thin and thick TE respectively. The wavy TE exhibits a lower magnitude vortex shedding at a frequency of 7.4 kHz which can be observed on the logarithmic representation in Figure 6 (right). With these frequencies, and the relative velocities and thicknesses available in Table 1, the Strouhal number can be approximated for all configurations (see Table 2). To assess the accuracy of the numerical approach, a dedicated experimental evaluation is conducted.

Table 2: Strouhal numbers derived from the vortex shedding frequencies observed in the CFD.

Thin straight TE	Thick straight TE	Wavy TE
$0.11 < St < 0.16$	$0.19 < St < 0.23$	$0.11 < St < 0.15$

EXPERIMENTAL EVALUATION

The experimental approach consists in assessing the compressor in isolation. The three configurations were prototyped using stereolithography (SLA) (see Figure 7). The prototypes were balanced and tested using the same motor and housing.
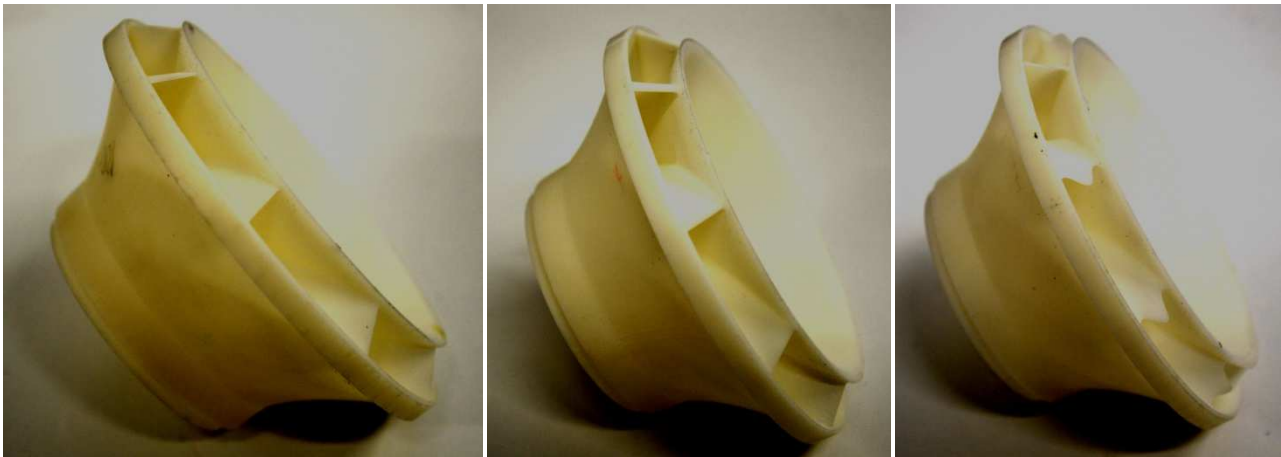
Figure 7: SLA prototype of (left) the thin TE, (middle) the thick TE and (right) the wavy TE.

The measurements of the compressors in isolation were performed using a dedicated aeroacoustic set-up following the ISO standards for aerodynamic performance and acoustics measurements in-duct [13, 14]. This set-up comprises of an orifice plate to measure the flow rate and an outlet throttle to control it. Pressure taps and microphones fitted with nose cones are located upstream and downstream of the compressor placed in the middle section of the device. Aerodynamic performance and acoustic measurements are performed simultaneously. Two anechoic terminations are located at each end of the device to minimise reflection. Pictures of the set-up are shown in Figure 8. The measurements of the different configurations are shown in Figure 9.

Figure 8: Aeroacoustic set-up with (left) the outlet throttle, (middle) a microphone with its nose cone and (right) the full device with the orifice plate and one anechoic termination at the foreground.
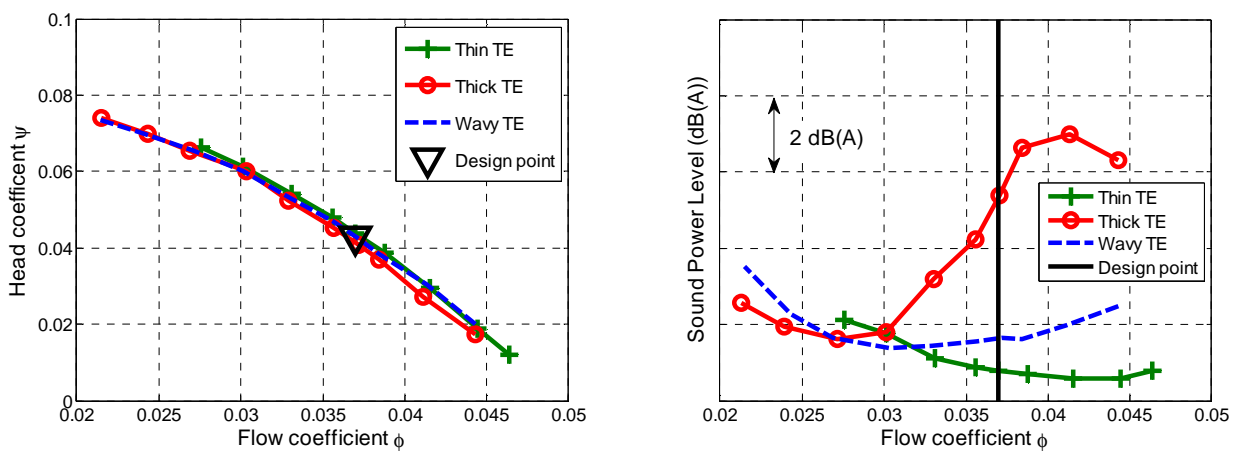

Figure 9: Aerodynamic performance (left) and sound power level (right) for different configurations.

Figure 9 (left) shows that the performance of the compressors remains fairly consistent reaching a maximum of 3.5% variation from the design point. From an acoustic perspective, the sound power

level generated by the thick TE is higher than the two other configurations at high flow coefficient. At the design point ($\phi = 0.037$) the wavy TE and the thick TE are louder than the thin TE by approximately 1 and 5 dB(A) respectively.

The aeroacoustic device has an internal diameter of 145 mm leading to a cut-on frequency of approximately 1.4 kHz. Above this cut-on frequency, the effect of the higher order mode may cause some inaccuracies, it is nevertheless interesting to analyse the frequency content of these signals. The narrow band analysis for a variety of flow rates is shown in Figure 10 for all configurations. For clarity each spectrum has been offset to emphasize the difference in signature amongst them.
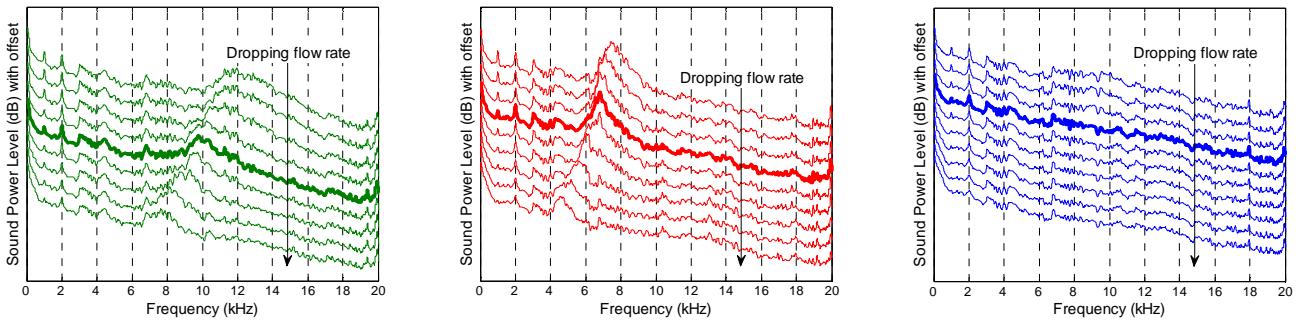

Figure 10: Acoustic spectra for a variety of flow rates for (left) the thin TE, (middle) the thick TE and (right) the wavy TE. The operational flow rate is highlighted using a thicker line. An offset of 10 dB is set between each flow rate.

As the rotational speed is kept constant the flow dependant lump of acoustic energy decreasing in frequency with decreasing flow rate can safely be interpreted as a vortex shedding. This feature is obvious for the thick TE and can be observed, to a lower extent, for the thin TE. Furthermore, the thick TE is exhibiting a lower frequency vortex shedding than the thin TE which is in line with the CFD prediction. The wavy TE doesn't show any vortex shedding feature.

At the operational flow rate, the vortex shedding frequencies are higher than that predicted by the CFD leading to higher Strouhal numbers (see Figure 11 and Table 3). It is interesting to note that the trend in terms of magnitude seems to be consistent with the CFD. The discrepancy in terms of vortex shedding frequency between the CFD and the experiment is not clearly understood. The DES CFD assumes a fully turbulent flow, which in the case of low Reynolds number may produce inaccuracies. A study of vortex shedding conducted by Ausoni, [15], has shown that by tripping the boundary layer, thus reaching a fully turbulent regime, can produce a 20% reduction in the vortex shedding frequency which could explain the difference between the CFD and the measurements.
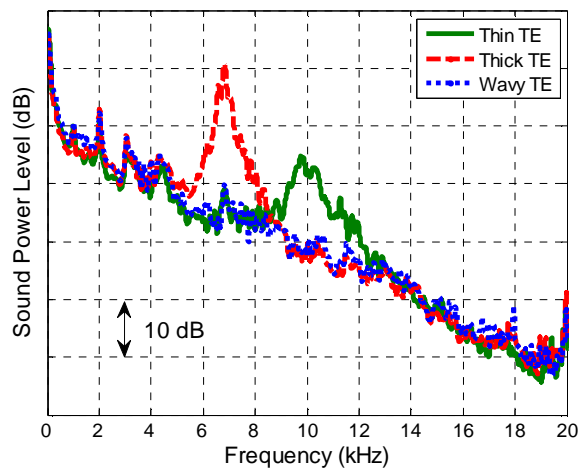

Figure 11: Acoustic spectra measured at operating flow rate for each configuration.

Table 3: Vortex shedding frequency and Strouhal number derived from measurements.

	Thin straight TE	**Thick straight TE**	**Wavy TE**
Vortex shedding frequency (Hz)	9800	6800	-
Strouhal number	$0.15 < St < 0.20$	$0.27 < St < 0.34$	-

The vortex shedding has been reduced using the wavy TE. The initial motivation for this work is to assess the influence of the trailing edge geometry on the sound quality. The acoustic signature induced by the vortex shedding generates a 'hissing' noise; consequently the improvement of the vortex shedding should be reflected in a lower sharpness.

Sharpness is a psychoacoustic metric which measures the high frequency content of a sound. A sound which is too 'sharp' will be perceived as aggressive. Sharpness is expressed in 'acum'. A value of 1 acum corresponds to the sharpness of a narrow band noise centred at 1 kHz, with a bandwidth equal to one critical band and a level of 60 dB, [16].

The sharpness has been measured on the outlet microphone for all configurations. Measurements have been carried out for a constant speed and a variety of flow rates and for a constant restriction and a variety of running speeds. The former is complementing the information given by the sound power level (see Figure 9 (right)) and the latter is representing the compressor as it will be used in the product. Both measurements are shown in Figure 12.
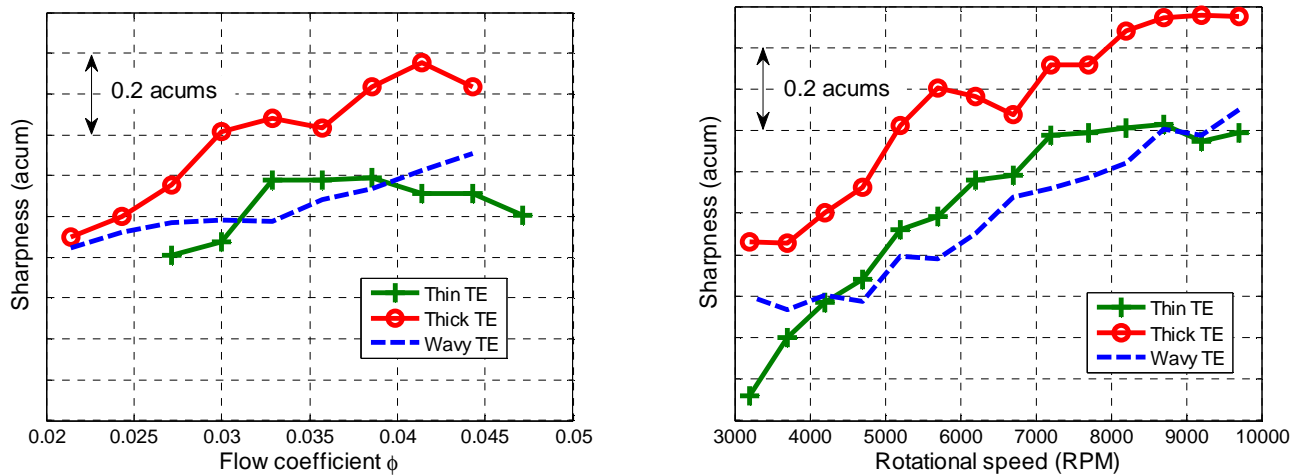

Figure 12: Sharpness for (left) a constant speed and (right) a constant restriction.

As expected it can be noticed that the thick TE exhibits a much larger sharpness than the two other designs. At the operational flow rate ($\phi = 0.037$), despite being slightly louder (see Figure 9 (right)), the wavy TE appears to sound marginally less sharp than the thin TE. For a given restriction, this observation is verified on a wide range of running speed ranging approximately from 4.5 to 8.5 kRPM.

CONCLUSION

An investigation on the influence of the trailing edge geometry on the noise generated by a low Reynolds number mixed flow compressor has been conducted. Three designs have been assessed for aerodynamic performance and acoustics using numerical and experimental methods. The three designs studied in this paper comprised of a thin straight TE, a thick straight TE and a 'wavy' (sinusoidal) TE.

A DES CFD simulation predicted the expected frequencies of the vortex shedding for all configurations. Despite exhibiting a similar trend to the experimental results, the vortex shedding frequency is underestimated by the CFD. Further work on modelling the boundary layer regime is suggested to improve the correlation between numerical and experimental approaches.

The measurements showed that the three trailing edge designs did not affect the aerodynamic performance. Out of the three designs, both straight trailing edge geometries were exhibiting strong vortex shedding.

A psychoacoustic metric, the sharpness, was used to assess the influence of the vortex shedding on the sound quality. Using this metric, the 'wavy' trailing edge appears to be the less sharp and should therefore be preferred over the straight trailing edge designs to potentially enhance the sound quality of the Dyson Air Multiplier^{TM} desk fan (to be verified throughout a dedicated jury evaluation study).

BIBLIOGRAPHY

[1]   L. Desvard, J. Hurault, M. A. B. Mohamed Zamzam and A. Symes, "An investigation on the effect of uneven blade spacing on the tonal noise generated by a mixed flow fan," in *Fan 2012*, Senlis, 2012.

[2]   H. Hopper, S. R. Voisey and W. Hunt, "Optimisation and implementation of a hybrid passive silencer for improved sound quality," in *Nois and vibration - Emerging technologies (NOVEM)*, Dubrovnik, 2015.

[3]   N. G. Fitton, F. Nicolas and P. D. Gammack, "Fan". United States of America Patent US 7931449 B2, 26 April 2011.

[4]   S. Pröbsting, "Coherent structures at the serrated trailing-edge of a NACA 0012," Delft University of Technology, Delft, 2011.

[5]   M. A. Zahari and S. S. Dol, "Application of vortex induced vibration energy generation technologies to the offshore oil and gas platform: The preliminary study," *International Journal of Mechanical, Aerospace, Industrial and Mechatronics Engineering,* vol. 8, no. 7, pp. 1313-1316, 2014.

[6]   S. Yarusevych, S. Pierre and J. Kawall, "On vortex shedding from an airfoil in low-Reynolds-number flows," *Journal of Fluid Mechanics,* vol. 632, pp. 245-271, 2009.

[7]   D. J. Moreau, L. A. Brooks and C. J. Doolan, "The effect of boundary layer type on trailing edge noise from sharp-edged flat plates at low-to-moderate Reynolds number," *Journal of Sound and Vibration,* vol. 331, no. 17, pp. 3976-3988, 2012.

[8]   D. J. Moreau, L. A. Brooks and C. J. Doolan, "On the noise reduction mechanism of a flat plate serrated trailing edge at low-to-moderate Reynolds number," in *18th AIAA/CEAS Aeroacoustics Conference*,

Colorado, 2012.

[9] D. H. Geiger, "Comparative analysis of serrated trailing edge designs on idealized aircraft engine fan blades for noise reduction," Virginia Tech, 2004.

[10] J. F. Braush, B. A. Janardan, J. W. Barter and G. E. Hoff, "Chevron exhaust nozzle for a gas turbine engine". United States of America Patent US 6360528 B1, 26 March 2002.

[11] K. Hayashi, H. Nishino, H. Hosoya, A. Matsuo and K. Karikomi, "Wind turbine blade and wind power generator using the same". United States of America Patent US8851857 B2, 7 October 2014.

[12] M. Shibata, T. Furukawa, Y. Hayashi and E. Kato, "Wind turbine provided with nacelle". United States of America Patent US 6830436 B2, 21 February 2003.

[13] ISO 5801, "Industrial fans - Performance testing using standardized airways," 2007.

[14] ISO 5136, "Acoustics - Determination of sound power radiated into a duct by fans and other air moving devices - In-duct method," 2003.

[15] P. Ausoni, M. Farhat, Y. Ait Bouziad, J. L. Kueny and F. Avellan, "Kármán vortex shedding in the wake of a 2D hydrofoil: Measurement and numerical simulation," in *Meeting of WG on Cavitation and Dynamic Problems in Hydraulic Machinery and Systems*, Barcelona, 2006.

[16] H. Fastl and E. Zwickers, Psychoacoustics: facts and models, Springe, 3rd ed., 2007.